

Road Genome: A Topology Reasoning Benchmark for Scene Understanding in Autonomous Driving

Huijie Wang¹,
Zhenbo Liu², Yang Li¹, Tianyu Li¹, Li Chen¹,
Chonghao Sima¹, Yuting Wang¹, Shengyin Jiang¹, Feng Wen²,
Hang Xu², Ping Luo¹, Junchi Yan¹, Wei Zhang², Jun Yao², Yu Qiao¹,
Hongyang Li¹,

WANGHUIJIE@PJLAB.ORG.CN

LIHONGYANG@PJLAB.ORG.CN

¹OpenDriveLab, Shanghai AI Laboratory ²Noah's Ark Lab, Huawei

<https://github.com/OpenDriveLab/OpenLane-V2>

Abstract

Understanding the complex traffic environment is crucial for self-driving vehicles. Existing benchmarks in autonomous driving mainly cast scene understanding as perception problems, e.g., perceiving lanelines with vanilla detection or segmentation methods. As such, we argue that the perception pipeline provides limited information for autonomous vehicles to drive in the right way, especially without the aid of high-definition (HD) map. For instance, following the wrong traffic signal at a complicated crossroad would lead to a catastrophic incident. By introducing **Road Genome (OpenLane-V2)**, we intend to shift the community's attention and take a step further beyond perception - to the task of topology reasoning for scene structure. The goal of Road Genome is to understand the scene structure by investigating the relationship of perceived entities among traffic elements and lanes. Built on top of prevailing datasets, the newly minted benchmark comprises 2,000 sequences of multi-view images captured from diverse real-world scenarios. We annotate data with high-quality manual checks in the loop. Three subtasks compromise the gist of Road Genome, including the 3D lane detection inherited from OpenLane. We have/will host Challenges in the upcoming future at top-tiered venues.

Keywords: 3D Lane Detection, Traffic Element Recognition, Topology Reasoning, Scene Understanding, Autonomous Driving, Dataset and Benchmark

1. Introduction

In recent years, the availability of public large-scale datasets and benchmarks has greatly facilitated research on autonomous driving. A critical aspect would be understanding the complex driving environment, which is the prerequisite for reasonable decisions. Many datasets (Huang et al., 2019; Yan et al., 2022) focus on perceiving visible lanelines to keep vehicles on the right track, while others (Stallkamp et al., 2012; Fregin et al., 2018; Ertler et al., 2020) specify in acquiring traffic information through detecting traffic signals. Nevertheless, this separation of tasks represents a limited understanding of the driving scene. For instance, when driving into a crossroad without any visible laneline, an autonomous vehicle might wonder which direction to go. Also, when it sees a green light and decides to go into the intersection, chaos is unpreventable as the lane it follows is controlled by another red light. In this work, we try to build a strong association among traffic elements and lanes,

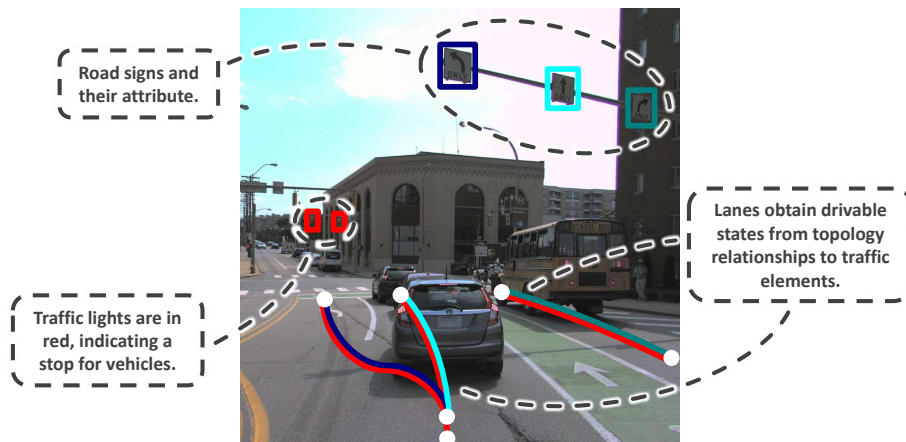


Figure 1: Road Genome (OpenLane-V2) comprises various types of annotations. Except for typical lanes and traffic elements as objects, the topology relationships are built to provide new challenges for the autonomous driving community.

aiming to create a topology of the physical world and thus facilitate decision-making in the downstream tasks.

To keep autonomous vehicles driving in the correct position, the concept of lanes is needed to be introduced. The perception of lanelines, which are the visible separation of lanes, is well explored. Previous datasets (Aly, 2008; Lee et al., 2017; Huang et al., 2019; Yu et al., 2020) annotate lanelines on images in the perspective view (PV). Such a 2D representation is insufficient to fulfill real-world requirements. It would lead to improper action decisions in the planning and control module in challenging scenarios, *e.g.*, uphill/downhill, bump, and crush turn. Recent works (Chen et al., 2022b; Yan et al., 2022) define lanelines in the 3D space but still limit the labeling range within the front view image. Besides, serving as separations of neighboring lanes, the visible lanelines might not benefit downstream tasks directly. In common circumstances, vehicles follow the center of lanes, *i.e.*, lane centerlines, to drive on the road. To generate this type of invisible and conceptual trajectories, post-processing techniques can be applied. But when it comes to an absence of lanelines, such as at a crossroad where there is usually no marking, the desired trajectory remains empty and vehicles do not have any guidance to refer to.

Similarly, the perception of traffic signals is formulated as a typical 2D detection problem in PV. Though traffic elements on the roads, such as traffic lights and road signs, provide practical and real-time information, existing formulations (Fregin et al., 2018; Ertler et al., 2020) do not provide correct information for a certain car. The reason is that one traffic signal controls one or several lanes according to the predefined traffic rules. As all the traffic elements at a scene are detected simultaneously, autonomous vehicles might get confused about which to obey.

In this work, we seek to unify the abovementioned tasks and provide an ideal understanding of driving scenes that promotes downstream tasks directly. To this end, we propose Road Genome to shed light on the task of **scene structure perception and reasoning**. The requirement of perception is to obtain correct information from the captured scenes, while reasoning defines the topology relationships of perceived entities to generate a reasonable understanding of the environment.

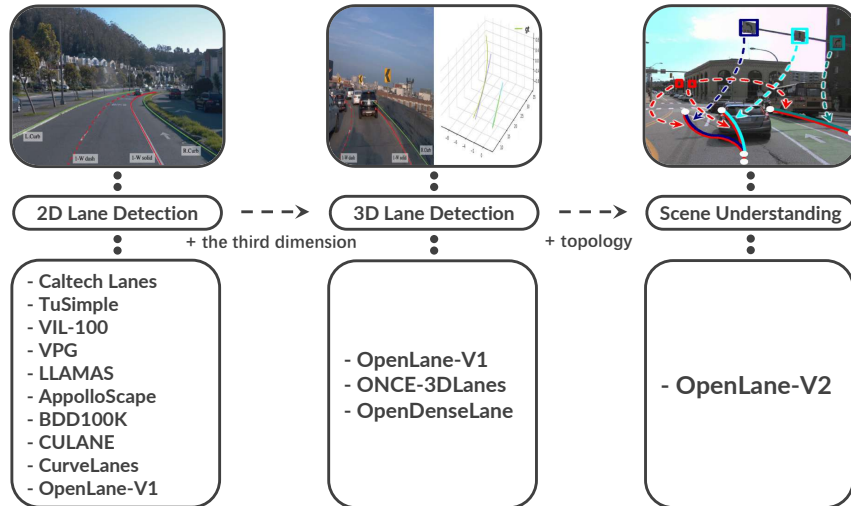


Figure 2: Roadmap of lane detection datasets. Most of the previous works provide only 2D labels. Benefiting from the pioneering OpenLane dataset (Chen et al., 2022a), lane annotations in 3D space have gained popularity in recent years. Taking one step further, Road Genome (OpenLane-V2) includes topology relationships to promote the task of scene understanding.

Inherited from the OpenLane dataset (Chen et al., 2022a), which is the first real-world and large-scale 3D lane dataset, **Road Genome**, also known as **OpenLane-V2**, provides lane annotations in 3D space to reflect their properties in the real world. The directed lane centerlines and their connectivity serve as map-like perception results to facilitate downstream tasks. Additional to the annotations of traffic elements, we establish relationships between lanes and traffic elements. That is, the connection between a lane and a traffic element is denoted as valid if and only if the traffic element controls the lane. With these representations, autonomous vehicles understand the current driving scenarios of where to go or whether to accelerate or slow down (Figure 1). For more details on the proposed dataset, please refer to Section 3.

For the newly defined task, we strive to make our metric capable of covering all aspects of the task. The **OpenLane-V2 Score (OLS)** summarizes model performances with its component of DET and TOP for perception and reasoning respectively. Section 4 gives an exhaustive description of the proposed tasks and metrics.

Our contributions are as follows:

- We present the Road Genome dataset for benchmarking the task of scene understanding. To the best of our knowledge, Road Genome is the first dataset that focuses on topology reasoning in the autonomous driving domain.
- Building on top of awesome benchmarks, Road Genome includes massive images collected from various cities worldwide. It contains 2.1M instance-level annotations and 1.9M positive topology relationships. All annotations are carefully validated.
- We provide a development kit for easy access to the proposed dataset. Besides, plugins to prevail deep learning frameworks for training models would be jointly main-

Dataset	#Img.	#Cls.	#Anno.	Resolution	Region
LaRA (De Charette and Nashashibi, 2009)	11K	4	9K	640×480	France
Stereopolis (Belaroussi et al., 2010)	847	4	251	960×1080	France
GTSRB (Stallkamp et al., 2012)	5K	43	39K	1360×1024	Germany
LISA (Mogelmose et al., 2012)	6K	49	7K	1280×960	USA
GTSDb (Houben et al., 2013)	900	43	1K	1360×800	Germany
BelgiumTS (Timofte et al., 2014)	9K	62	13K	1628×1236	Belgium
RTSD (Shakhuro and Konouchine, 2016)	179K	156	104K	-	Russia
TT100K (Zhu et al., 2016)	100K	221	26K	2048×2048	China
BSTLD (Behrendt et al., 2017)	13K	15	24K	1280×720	USA
JAAD (Rasouli et al., 2017)	82K	-	378K	1920×1080	Worldwide
DTLD (Fregin et al., 2018)	-	344	230K	2048×1024	Germany
MTSD (Ertler et al., 2020)	100K	313	325K	-	Worldwide
Road Genome (OpenLane-V2)	466K	13*	258K*	-	Worldwide

Table 1: Comparison of current traffic element datasets. #Img., #Cls., and #Anno. denote the number of images, classes, and annotations respectively. * We decompose semantic meanings of traffic elements into base attributes and omit elements that require OCR to acquire their semantic meaning for vision-centric perception.

tained with the community. The test server and leaderboard will also be maintained for fair comparisons.

2. Related Work

2.1 3D Lane Detection

The task of lane detection has been pursued for several years (Figure 2). Previous works (Aly, 2008; Wu and Ranganathan, 2012; Lee et al., 2017; TuSimple, 2017; Behrendt and Soussan, 2019; Xu et al., 2020) provided 2D laneline annotations in PV. CULANE (Pan et al., 2018) collected a large scale of data and manually annotated the occluded lane markings with cubic splines. With multiple sensors, AppolloScape (Huang et al., 2019) included per-pixel lane mark labeling in 35 classes. BDD100K (Yu et al., 2020) labeled lanes attributes of continuity (full or dashed) and direction (parallel or perpendicular) on a massive amount of data. However, the scope of annotation is still limited in the 2D space on front-view images. OpenLane (Chen et al., 2022a) was the first large-scale, real-world 3D laneline dataset. It is equipped with a wide span of diversity in both data distribution and task applicability. In the spirit of it, the proposed Road Genome provides annotations in 3D space. Instead of the visible lanelines, its annotations of conceptual lane centerlines serve as trajectories for downstream tasks. Moreover, as human drivers also observe situations from backward, we provide lane annotations in all directions of the ego car within a long range.

2.2 Traffic Element Recognition

Over the last decade, existing datasets have annotated traffic elements on images from the driving scenarios. Table 1 summarizes the relevant counterparts. Most of the works in the early 2010s comprised a small amount of data (Belaroussi et al., 2010; Stallkamp et al., 2012; Mogelmose et al., 2012; Houben et al., 2013; Timofte et al., 2014). GTSRB (Stallkamp et al., 2012) collected data from multiple German landscapes and showed that neural networks

Dataset	Purpose
Kooij et al. (2014)	Future behavior of pedestrians
JAAD (Rasouli et al., 2017)	Behavior of pedestrians at crosswalk
HDD (Ramanishka et al., 2018)	Driver behavior & causal reasoning
Kooij et al. (2019)	Future behavior of cyclists
Road Status Graph (Tian et al., 2020)	Pairwise relationships of moveable objects
Road Genome (OpenLane-V2)	Scene structure understanding

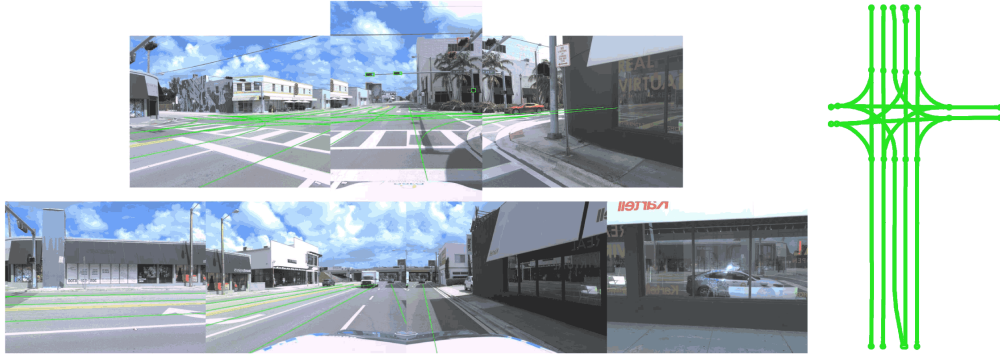
Table 2: Existing datasets on scene understanding. Previous datasets focus on understanding the behavior or relationship of moveable objects. Ours study topology relationships of driving scenes, which could provide trajectories for downstream tasks.

could outperform human test persons in detecting traffic signs. MTSD (Ertler et al., 2020) made a step forward in both scale and diversity that contained 100K street-level images worldwide from diverse scenes, geographical locations, and varying weather and lighting conditions. JAAD (Rasouli et al., 2017) provided a high-level analysis of traffic scenes. It includes not only bounding boxes but also behavioral and contextual annotations for the scenes, which allows research on understanding pedestrian intention. Though with dedicated labels, previous datasets are limited in the understanding of traffic elements that neglect their relationships to lanes that vehicles are driving on. We provide additional annotation on topology relationships of presented objects, which enable autonomous vehicles to have an understanding of the driving environment.

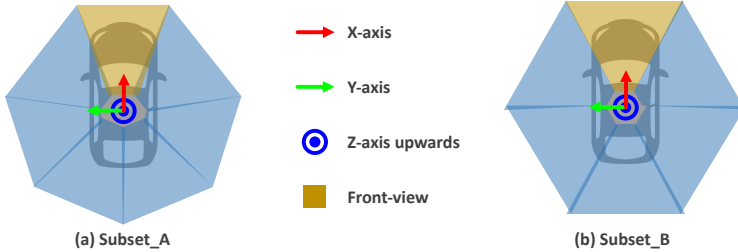
2.3 Scene Understanding

Understanding the complex driving scene plays a vital role in autonomous driving, especially in complicated scenarios. Few datasets focus on the comprehension of captured scenes. With a wide variety of predicates, current datasets (Lu et al., 2016; Krishna et al., 2017; Hudson and Manning, 2019; Kuznetsova et al., 2020) encompassed 2D images on which there are only a small amount of objects. Datasets in the human-object interaction domain (Gupta and Malik, 2015; Chao et al., 2018) limited the labeled relationship to the interactions between human beings and detected objects. The aforementioned datasets include annotations such as “cat-ride-snowboard”, which are relationships between spatially-closed objects. However, in our case, a traffic light may correspond to a lane in the distance rather than a closer one. To predict the correct relationships, models are required to have an understanding of the predefined traffic rules.

In the field of autonomous driving, most of the previous works try to understand the intension of perceived entities (Table 2). Tian et al. (2020) provided pairwise relationships between moveable objects, *e.g.*, vehicles and pedestrians. Other datasets paid attention to the intention of driver (Ramanishka et al., 2018; Kooij et al., 2019) or non-driver (Kooij et al., 2014; Rasouli et al., 2017) agents. With the emergence of occupancy and occupancy flow, the object-level representation of foreground objects becomes less popular. As demonstrated by Hu et al. (2023), planning is of vital importance in autonomous driving. In the proposed dataset, we emphasize the understanding of the background, which serves as a complement to occupancy and could generate trajectories for downstream tasks.



(a) Example from *subset_A*. Multi-view images (left) covering a fully panoramic FOV are provided for each frame. We depict centerlines of the frame in BEV on the right side.



(b) Coordinate systems are aligned between two subsets. Though containing a different number of cameras, both subsets provide multi-view images covering 360° horizontal FOV.

Figure 3: Sensor setups of the Road Genome dataset. Centerlines are annotated in all directions within a specific range, while traffic elements are annotated only on the front-view images.

3. Road Genome (OpenLane-V2)

In this section, we give an overview of the proposed dataset, which is publicly available in our repository. Building on top of the Argoverse 2 (Wilson et al., 2023) and nuScenes (Caesar et al., 2020) datasets, Road Genome includes images in 2,000 segments collected worldwide under different challenging environments, including noon and night, sunny and rainy days, downtown and suburbs. Through a dedicated labeling process, we encompass high-quality annotations for perception and reasoning.

3.1 Data

The sensor setups differ as the included image data is collected from different sources. As a result, the dataset is divided into two subsets, namely *subset_A* and *subset_B*. The *subset_A* contains images from 7 cameras in the resolution (height \times width) of 1550×2048 , in which the front-view images are transposed as 2048×1550 to improve the vertical FOV, while all images in *subset_B* are from 6 cameras and in the resolution of 900×1600 . Despite the difference in camera settings, images in a single frame cover the fully panoramic FOV (Figure 3a). We unify setups into the same format for all possible fields, such as the coordinate system. All coordinate systems are right-handed such that for ego coordinate (Figure 3b), the x-axis is positive forwards, the y-axis is positive to the left, and the z-axis

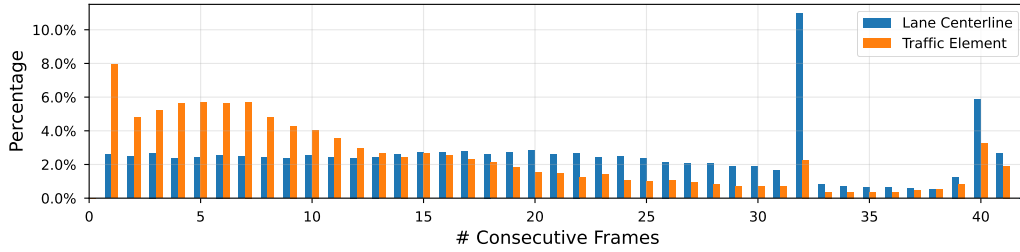
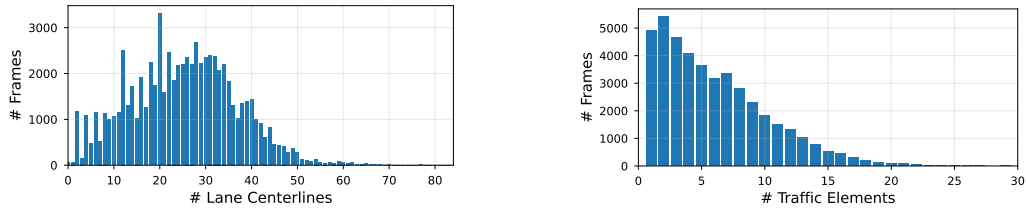
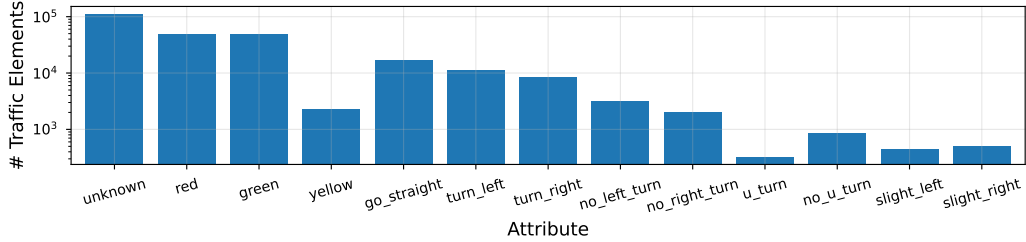


Figure 4: Most of the instances are presented in several consecutive frames. The outliers on the right side are due to the fact that the maximum number of frames for a single segment lay in these numbers on different subsets.



(a) Distribution of the number of centerlines in each frame.

(b) Distribution of the number of traffic elements in each frame.



(c) Distribution of the number of traffic elements in different categories over the dataset.

Figure 5: The number of centerlines and traffic elements is up to 80 and 30 in a single frame respectively. The category distribution of traffic elements is highly imbalanced.

is positive upwards. Camera intrinsics, extrinsic, and 6-DOF ego-vehicle pose in the global coordinate system are provided.

3.2 Annotation

With the help of experienced annotators and multiple validation stages, we provide high-quality annotations for the Road Genome dataset. Annotations are provided at $2Hz$ and temporal-consistent (Figure 4). For a single instance, which presents in different frames, its *id* is kept the same through different frames. Detailed statistics for each subset can be found in the repository.

3.2.1 LANE CENTERLINE

We provide 3D annotations for the lane centerline. The ego car locates at $(0, 0, 0)$ for each frame, and a lane centerline is represented by an ordered list of points in the 3D space. Specifically, for a lane centerline $[p_1, \dots, p_n]$, $p_1 = (x_1, y_1, z_1)$ describe the starting point of

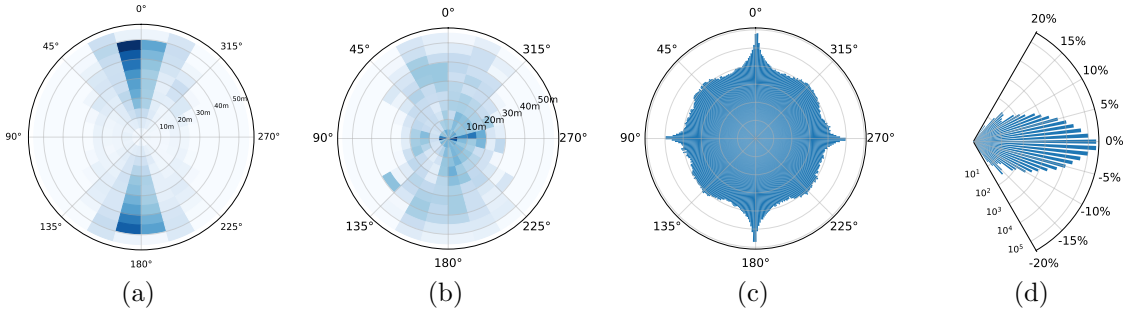


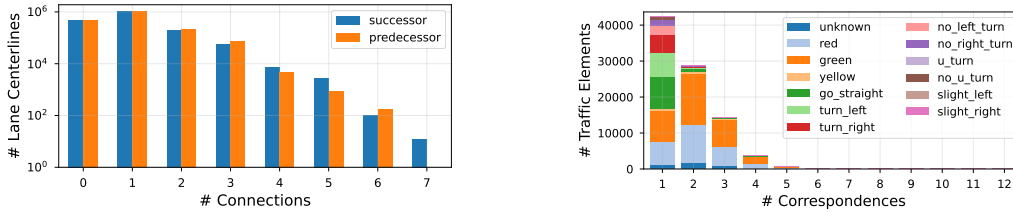
Figure 6: (a) Most lanes are located in the front or back side of the ego vehicle. As the darker color denotes the larger average length of centerlines in (b), centerlines on both sides of the car are typically longer. The histograms of (c) and (d) are in the log scale. The direction (c) and slope (d) of centerlines depict symmetric patterns.

the lane and $p_n = (x_n, y_n, z_n)$ is the ending point. As the original data of *subset_B* exclude the height information, we set values of the z-axis to 0. The direction of a centerline, from the starting point to the ending point, denotes that a vehicle should follow the direction when driving on this lane based on the predefined traffic rules. Note that we set n to 201 in the given data, but we subsample 11 points for each lane for efficient evaluation. We annotate all existing lane centerlines within the defined range. The range is limited within $[-50m, +50m]$ along the x-axis and $[-25m, +25m]$ along the y-axis. As we provide annotations on traffic elements and topology relationships, which provide lanes with semantic attributes, all lanes are in the same class.

Statistically, about 90% of frames have more than 10 lane centerlines while about 10% have more than 40 (Figure 5a). Figure 6 depicts the statistics on lane centerlines. Most of the lanes locate in the distance along the same or opposite direction of the ego vehicle since there are intersections with some short lanes in many segments. Lanes with a relatively greater length usually lay close to the ego car, as there are several lanes in the same or opposite direction in a road. As for the direction and slope of lanes, they are evenly distributed.

3.2.2 TRAFFIC ELEMENT

All presented traffic elements, whose sizes in pixels exceed a certain threshold, on the front-view images are labeled. A traffic element is denoted as a 2D bounding box (x_1, y_1, x_2, y_2) , where (x_1, y_1) is the top-left corner and (x_2, y_2) is the bottom-right corner. The semantic meaning of traffic elements is marked as an attribute of the traffic elements. For unreadable or irrelevant elements, their attributes are set to unknown. We annotate 13 attributes, namely *unknown*, *red*, *green*, *yellow*, *go_straight*, *turn_left*, *turn_right*, *no_left_turn*, *no_right_turn*, *u_turn*, *no_u_turn*, *slight_left*, and *slight_right*. Note that we decompose a traffic element with two or more attributes into several identical bounding boxes with different labels. For instance, a road sign, which is at the position of (x_1, y_1, x_2, y_2) and with the meaning of “go straight and turn left”, is divided into two bounding boxes, namely $(x_1, y_1, x_2, y_2, go_straight)$ and $(x_1, y_1, x_2, y_2, turn_left)$.



(a) Most centerlines have one predecessor or successor. But some have several, which often happen at intersections.

(b) Most traffic elements control a small number of centerlines, while a few, which are usually traffic lights, control more.

Figure 7: Topology relationships are complex in a single frame, as an entity can be connected or corresponded to a different number of instances.

Figure 5b and 5c describes the distribution of traffic elements. Due to the nature of traffic element configurations, several types of elements are extremely rare, such as *u_turn*, which only takes up 0.1% of the total number. The class imbalance problem would be encouraged to be studied.

3.2.3 TOPOLOGY

Two types of topology relationships are emphasized in the proposed dataset. The connectivity among lane centerlines builds up trajectories for autonomous vehicles to follow. As a lane is directed and represented as a list of points, the connection of two lanes means that the ending point of a lane is connected to the starting point of another lane. We decompose a continuous lane into two lanes if and only if in the cases of intersection, fork, and merge, resulting in multiple successors of predecessors for a single centerline (Figure 7a). The correspondence of a lane and a traffic element indicates that a driver needs to obey the traffic signals when driving in this lane. As we need to check the traffic lights and road markers simultaneously when driving, a lane can be controlled by an arbitrary number of traffic elements (Figure 7b).

4. Task Definition & Evaluation Metric

In this section, we introduce the tasks and metrics in Road Genome (OpenLane-V2). The primary task of the dataset is scene structure perception and reasoning, which requires the model to recognize lanes and their dynamic drivable states in the surrounding environment. The challenge includes detecting lane centerlines and traffic elements and recognizing the attribute of traffic elements and topology relationships on detected objects. We further divide the primary task into three subtasks: 3D lane detection, traffic element recognition, and topology recognition. The OpenLane-V2 Score (OLS), which is the average of various metrics from different subtasks, is defined to describe the overall performance of the primary task:

$$\text{OLS} = \frac{1}{4} \left[\text{DET}_l + \text{DET}_t + f(\text{TOP}_{ll}) + f(\text{TOP}_{lt}) \right]. \quad (1)$$

4.1 3D Lane Detection

In the spirit of the OpenLane dataset (Chen et al., 2022a), which is the first real-world and the largest scaled 3D lane dataset to date, we provide lane annotations in 3D space. We define the subtask of 3D lane detection as perceiving directed 3D lane centerlines from the given multi-view images covering a fully panoramic FOV.

Given a pair of curves, namely a ground truth $v_l = [p_1, \dots, p_n]$ and a prediction $\hat{v}_l = [\hat{p}_1, \dots, \hat{p}_k]$, their geometric similarity is measured by the discrete Fréchet distance (Eiter and Mannila, 1994). Specifically, a coupling L is defined as a sequence of pairs between points in v and \hat{v} :

$$(p_{a_1}, \hat{p}_{b_1}), \dots, (p_{a_m}, \hat{p}_{b_m}), \quad (2)$$

where $1 = a_1 \leq a_i \leq a_j \leq a_m = n$ and $1 = b_1 \leq b_i \leq b_j \leq b_m = k$ for all $i < j$. Then the norm $\|L\|$ of a coupling L is defined as the distance of the most dissimilar pair in L . The Fréchet distance of a pair of curves is the minimum norm of all possible coupling that:

$$D_{\text{Fréchet}}(v_l, \hat{v}_l) = \min\{\|L\| \mid \forall \text{ possible } L\}. \quad (3)$$

We define a threshold $t \in \mathbb{T}$ that a pair of centerlines would be regarded as unmatched if their distance is greater than t . Then DET_t is averaged over match thresholds of $\mathbb{T} = \{1.0, 2.0, 3.0\}$:

$$\text{DET}_t = \frac{1}{|\mathbb{T}|} \sum_{t \in \mathbb{T}} AP_t. \quad (4)$$

Note that as the defined annotation range is relatively large compared to previous datasets, accurate perception of lanes in the distance would be hard. Thus, the match thresholds are relaxed for centerlines at a distance based on the distance between the ground truth lane and the ego car. For instance, a lane at a distance would be thresholded on $1.2t$ while another lane in a closer region would be thresholded on $1.1t$ for a same threshold $t \in \mathbb{T}$.

4.2 Traffic Element Recognition

Traffic elements and their attribute provide crucial information for autonomous vehicles. The attribute represents the semantic meaning of a traffic element, such as the red color of a traffic light. In this subtask, on the given image in the front view, the location of traffic elements and their attributes are demanded to be perceived simultaneously. Compared to typical 2D detection datasets, the challenge is that the size of traffic elements is tiny due to the large scale of outdoor environments.

To preserve consistency to the distance mentioned above, we modify the common IoU (Intersection over Union) measure as a distance that:

$$D_{\text{IoU}}(v_t, \hat{v}_t) = 1 - \frac{|v_t \cap \hat{v}_t|}{|v_t \cup \hat{v}_t|}, \quad (5)$$

where v_t and \hat{v}_t is the ground truth and predicted bounding box respectively. We consider IoU distance as the affinity measure with a match threshold of 0.75. The DET_t score is utilized to measure the performance of traffic elements detection and is averaged over different attributes \mathbb{A} that:

$$\text{DET}_t = \frac{1}{|\mathbb{A}|} \sum_{a \in \mathbb{A}} AP_a. \quad (6)$$

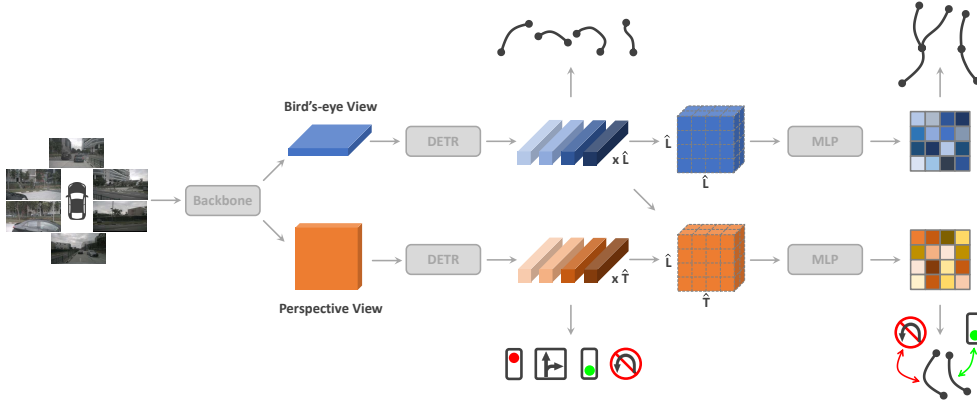


Figure 8: The baseline aggregate three subtasks into a single model. We adopt modules from previous networks to standardize inputs and outputs. Sophisticated designs, such as the introduction of temporal information and the interaction of features, are encouraged to be investigated in future works.

4.3 Topology Recognition

We first define the task of recognizing topology relationships in the field of autonomous driving. On the perceived entities, the topology relationships are built. For simplicity, we divide the graph on all entities into two subgraphs. The connectivity of directed lanes establishes a map-like network and is denoted as the lane graph (V_l, E_{ll}) . Note that the edge set $E_{ll} \subseteq V_l \times V_l$ is asymmetric, as the incoming and outgoing edges of a lane represent the connection on its starting and ending points respectively. An entry (i, j) in E_{ll} is positive if and only if the ending point of the lane v_i is connected to the starting point of v_j . Besides, the undirected graph $(V_l \cup V_t, E_{lt})$ describes the correspondence between centerlines and traffic elements. It can be seen as a bipartite graph that positive edges only exist between V_l and V_t .

The TOP score, which is an mAP metric adapted from the graph domain, is utilized to evaluate model performance. Specifically, given a ground truth graph $G = (V, E)$ and a predicted one $\hat{G} = (\hat{V}, \hat{E})$, we first build a projection on predicted vertices according to the entity-specific similarity measures, namely Fréchet and IoU distances for centerlines and traffic elements. The resulting vertex set \hat{V}' needs to fulfill the requirements such that $V = \hat{V}'$ and $\hat{V}' \subseteq \hat{V} \cup \{v_d\}$, where v_d is dummy vertices for unmatched vertices and have no neighbor. Positive edges are those whose confidence is greater than 0.5. Then the TOP score is the averaged mAP between (V, E) and (\hat{V}', \hat{E}') over all vertices:

$$\text{TOP} = \frac{1}{|V|} \sum_{v \in V} \frac{\sum_{\hat{n}' \in \hat{N}'(v)} P(\hat{n}') \mathbb{1}(\hat{n}' \in N(v))}{|N(v)|}, \quad (7)$$

where $N(v)$ denotes the ordered list of neighbors of vertex v ranked by confidence and $P(v)$ is the precision of vertex v in the ordered list. The TOP_{ll} is for topology among centerlines on graph (V_l, E_{ll}) , and the TOP_{lt} is for topology between lane centerlines and traffic elements on graph $(V_l \cup V_t, E_{lt})$.

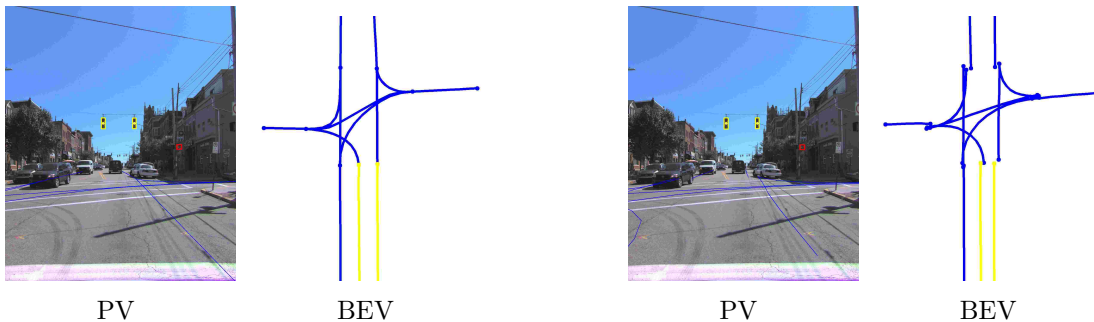


Figure 9: The left column is the ground truth, and the right is the prediction. The model predicts centerlines and their connectivity precisely. The correspondence between centerlines and traffic elements is described by colors in the BEV, and the two centerlines are also assigned with the correct semantic information.

5. Baseline

In this section, we provide a baseline model on our dataset, which aggregates all subtasks in a single model. Brief analyses and visualizations of the results are presented. The source code is publicly available in our repository.

5.1 Architecture

The model architecture is shown in Figure 8. Following the common practice in camera-based models (Chen et al., 2022a; Li et al., 2022a,b, 2023), an image backbone and view transformation module converts input images into bird’s-eye view (BEV) space. As the 2D annotations of traffic elements exist only in front-view images, a feature map in PV is produced as an auxiliary output. The resulting feature maps are one in BEV and one in PV. Two detection heads with the same DERT-like architecture are adopted. A reason is that, for detecting lanes extending the whole BEV feature, a global receptive field is preferred. Besides, to reason about the topology relationships between the perceived entities, the following modules require instance-level representations of the perception results to establish pairwise relationships.

Assuming the aforementioned network produces \hat{L} centerlines and \hat{T} traffic elements, to recognize their relationships, the topology heads take all possible pairs as input. We duplicate and concatenate the query features to form two grids in the shape of $\hat{L} \times \hat{L}$ and $\hat{L} \times \hat{T}$ for the relationship among lanes and between lanes and traffic elements respectively.

5.2 Supervision

Similar to DETR-like networks, the predicted centerlines and traffic elements are supervised by detection loss based on the Hungarian algorithm (Kuhn, 1955). As for topology relationships, the ground truth is represented as adjacent matrices in the shape of $L \times L$ and $L \times T$. Based on the matching results, ground truth is transformed into the same shape of predictions. Then the task of topology recognition is formulated as a binary classification problem on the given grids. Trained in an end-to-end manner, the resulting model is

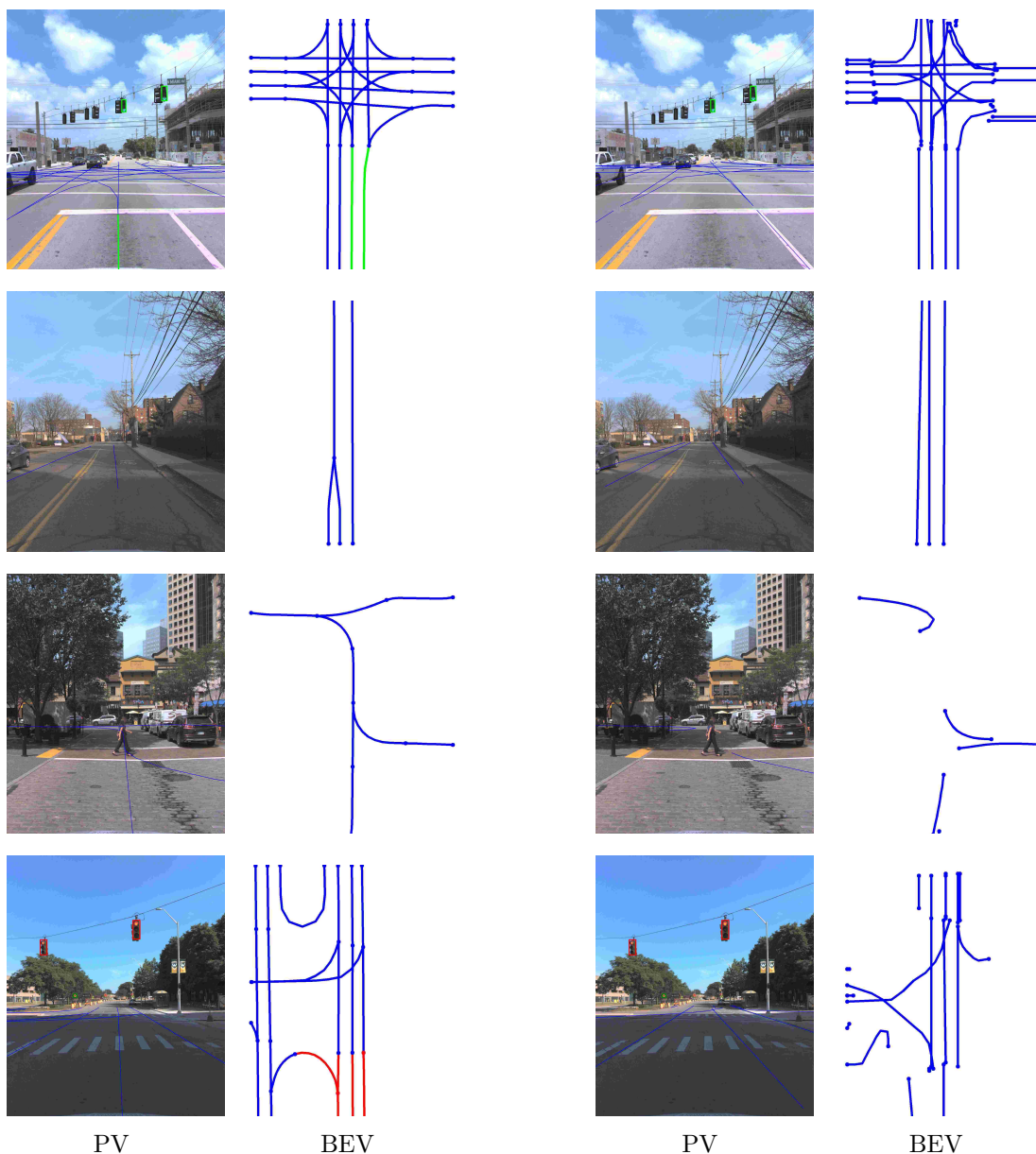


Figure 10: Although the baseline model is capable of making some correct predictions, in most cases, it still fails to generate reasonable results.

supervised by multiple signals: perception of lanes and traffic elements on two DETR heads and topology reasoning on two topology heads.

5.3 Analysis

Our baseline model is able to provide satisfactory predictions. As depicted in Figure 9, the predicted result is visually matched to the ground truth that the position, semantic, and connectivity of centerlines are correct. Note that there are three traffic lights in the front-

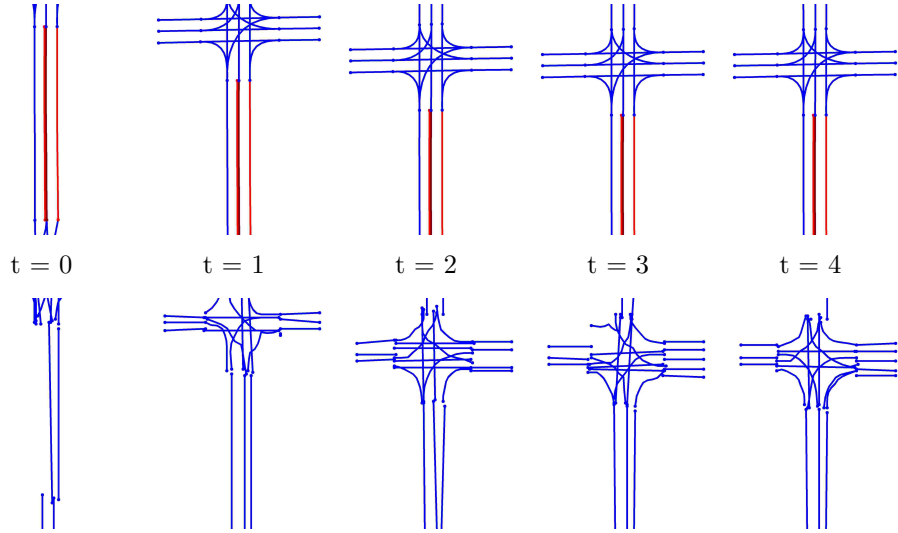


Figure 11: The upper row is the ground truth, and the lower is the prediction. Though the ego vehicle stays stationary in the last three frames, predictions of the model vary from frame to frame.

view image, two in yellow and one in red, but both centerlines in the BEV are associated with the yellow ones, indicating the model is capable of understanding the correspondence between lanes and traffic elements.

Yet the simplicity of the baseline model still limits its performance. Figure 10 reveals some failure cases. In the first row, the ego vehicle is located in a typical intersection. Though the symmetric lane structure is crystal clear for humans, the model even fails to perceive four lanes in each direction outside the crossing. The situation is the same for the scene in the second row. The model predicted three centerlines instead of two, which might be confused by the merging of two lanes behind the ego car. As for some complex shapes of lanes in the third row, only several short sections without any connection are produced. Incorrect perception of centerlines leads to a wrong understanding of the scenes. In the fourth row, the model provides an imperfect perception of lanes, in which the correspondence between lanes and traffic lights is missing. Moreover, temporal information plays a vital role in our task. Figure 11 describes a scenario with five consecutive frames. As the crossroad appears at $t = 1$, the predicted structures vary in the subsequent frames. Especially in the last three frames, in which the vehicle remains stationary, the predicted intersections do not follow the same pattern. This oscillation is unsatisfactory for real-world applications. Thus, temporal consistency is necessary for the model design to ensure stable predictions.

Besides, the baseline model only serves as a starter code for our tasks, so complicated designs are ignored. The instance-based query design is a trivial way to model pairwise relationships that complex object-specific representation might be attempted. It is also apparent to first predict instances and then determine their relationships. However, the positional or semantic information of one type of entity might be utilized to refine the prediction of the other type, which means that sequential inference could also be beneficial. Moreover, the model is trained in an end-to-end fashion for efficiency concerns, but a multi-stage or multi-task training strategy is also recommended.

6. Building OpenLane Community

One year ago, we announced the world’s first 3D laneline dataset, OpenLane. In this paper, we have brought another dataset with a unique scene structure perception and reasoning task. Based on these works, we invite you to join our community to pursue a higher level of autonomous driving technique. Going beyond our open-source codebases of OpenLane^{1,2} and Road Genome (OpenLane-V2)³, we are planning to host various competitions and relevant activities. Please stay tuned on our website⁴ for up-to-date information.

Changelog

Apr. 2023: initial manuscript released.

Mar. 2023: the first edition of OpenLane competition⁵ launched.

Feb. 2023: dataset v1.0: *subset_A* released; baseline model released.

Jan. 2023: dataset v0.1: samples released; devkit v0.1.0 released.

References

- Mohamed Aly. Real time detection of lane markers in urban streets. In *2008 IEEE intelligent vehicles symposium*. IEEE, 2008. 2, 4
- Karsten Behrendt and Ryan Soussan. Unsupervised labeled lane markers using maps. In *Int. Conf. Comput. Vis. Worksh.*, 2019. 4
- Karsten Behrendt, Libor Novak, and Rami Botros. A deep learning approach to traffic lights: Detection, tracking, and classification. In *ICRA*. IEEE, 2017. 4
- Rachid Belaroussi, Philippe Foucher, Jean-Philippe Tarel, Bahman Soheilian, Pierre Charbonnier, and Nicolas Papanoditis. Road sign detection in images: A case study. In *ICPR*. IEEE, 2010. 4
- Holger Caesar, Varun Bankiti, Alex H Lang, Sourabh Vora, Venice Erin Liong, Qiang Xu, Anush Krishnan, Yu Pan, Giancarlo Baldan, and Oscar Beijbom. nuscenes: A multimodal dataset for autonomous driving. In *CVPR*, 2020. 6
- Yu-Wei Chao, Yunfan Liu, Xieyang Liu, Huayi Zeng, and Jia Deng. Learning to detect human-object interactions. In *WACV*. IEEE, 2018. 5
- Li Chen, Chonghao Sima, Yang Li, Zehan Zheng, Jiajie Xu, Xiangwei Geng, Hongyang Li, Conghui He, Jianping Shi, Yu Qiao, et al. Persformer: 3d lane detection via perspective transformer and the openlane benchmark. In *ECCV*. Springer, 2022a. 3, 4, 10, 12
- Xiaolei Chen, Wenlong Liao, Bin Liu, Junchi Yan, and Tao He. Opendenselane: A dense lidar-based dataset for hd map construction. In *ICME*. IEEE, 2022b. 2

1. <https://github.com/OpenDriveLab/OpenLane>

2. https://github.com/OpenDriveLab/PersFormer_3DLane

3. <https://github.com/OpenDriveLab/OpenLane-V2>

4. <https://opendrive-lab.com>

5. <https://opendrive-lab.com/AD23Challenge.html>

- Raoul De Charette and Fawzi Nashashibi. Real time visual traffic lights recognition based on spot light detection and adaptive traffic lights templates. In *2009 IEEE Intelligent Vehicles Symposium*. IEEE, 2009. 4
- Thomas Eiter and Heikki Mannila. Computing discrete fréchet distance. 1994. 10
- Christian Ertler, Jerneja Mislej, Tobias Ollmann, Lorenzo Porzi, Gerhard Neuhold, and Yubin Kuang. The mapillary traffic sign dataset for detection and classification on a global scale. In *ECCV*. Springer, 2020. 1, 2, 4, 5
- Andreas Fregin, Julian Muller, Ulrich Krebel, and Klaus Dietmayer. The driveu traffic light dataset: Introduction and comparison with existing datasets. In *ICRA*. IEEE, 2018. 1, 2, 4
- Saurabh Gupta and Jitendra Malik. Visual semantic role labeling. *arXiv preprint arXiv:1505.04474*, 2015. 5
- Sebastian Houben, Johannes Stallkamp, Jan Salmen, Marc Schlipsing, and Christian Igel. Detection of traffic signs in real-world images: The german traffic sign detection benchmark. In *IJCNN*. Ieee, 2013. 4
- Yihan Hu, Jiazhi Yang, Li Chen, Keyu Li, Chonghao Sima, Xizhou Zhu, Siqi Chai, Senyao Du, Tianwei Lin, Wenhai Wang, et al. Planning-oriented autonomous driving. In *CVPR*, 2023. 5
- Xinyu Huang, Peng Wang, Xinjing Cheng, Dingfu Zhou, Qichuan Geng, and Ruigang Yang. The apolloscape open dataset for autonomous driving and its application. *IEEE TPAMI*, 42(10), 2019. 1, 2, 4
- Drew A Hudson and Christopher D Manning. Gqa: A new dataset for real-world visual reasoning and compositional question answering. In *CVPR*, 2019. 5
- Julian FP Kooij, Fabian Flohr, Ewoud AI Pool, and Dariu M Gavrila. Context-based path prediction for targets with switching dynamics. *International Journal of Computer Vision*, 2019. 5
- Julian Francisco Pieter Kooij, Nicolas Schneider, Fabian Flohr, and Dariu M Gavrila. Context-based pedestrian path prediction. In *ECCV*. Springer, 2014. 5
- Ranjay Krishna, Yuke Zhu, Oliver Groth, Justin Johnson, Kenji Hata, Joshua Kravitz, Stephanie Chen, Yannis Kalantidis, Li-Jia Li, David A Shamma, et al. Visual genome: Connecting language and vision using crowdsourced dense image annotations. *International journal of computer vision*, 123, 2017. 5
- Harold W Kuhn. The hungarian method for the assignment problem. *Naval research logistics quarterly*, 1955. 12
- Alina Kuznetsova, Hassan Rom, Neil Alldrin, Jasper Uijlings, Ivan Krasin, Jordi Pont-Tuset, Shahab Kamali, Stefan Popov, Matteo Mallocci, Alexander Kolesnikov, et al. The

- open images dataset v4: Unified image classification, object detection, and visual relationship detection at scale. *International Journal of Computer Vision*, 128(7), 2020. 5
- Seokju Lee, Junsik Kim, Jae Shin Yoon, Seunghak Shin, Oleksandr Bailo, Namil Kim, Tae-Hee Lee, Hyun Seok Hong, Seung-Hoon Han, and In So Kweon. Vpgnet: Vanishing point guided network for lane and road marking detection and recognition. In *ICCV*, 2017. 2, 4
- Hongyang Li, Chonghao Sima, Jifeng Dai, Wenhai Wang, Lewei Lu, Huijie Wang, Enze Xie, Zhiqi Li, Hanming Deng, Hao Tian, et al. Delving into the devils of bird’s-eye-view perception: A review, evaluation and recipe. *arXiv preprint arXiv:2209.05324*, 2022a. 12
- Tianyu Li, Li Chen, Xiangwei Geng, Huijie Wang, Yang Li, Zhenbo Liu, Shengyin Jiang, Yuting Wang, Hang Xu, Chunjing Xu, et al. Topology reasoning for driving scenes. *arXiv preprint arXiv:2304.05277*, 2023. 12
- Zhiqi Li, Wenhai Wang, Hongyang Li, Enze Xie, Chonghao Sima, Tong Lu, Yu Qiao, and Jifeng Dai. Bevformer: Learning bird’s-eye-view representation from multi-camera images via spatiotemporal transformers. In *ECCV*. Springer, 2022b. 12
- Cewu Lu, Ranjay Krishna, Michael Bernstein, and Li Fei-Fei. Visual relationship detection with language priors. In *ECCV*. Springer, 2016. 5
- Andreas Mogelmoose, Mohan Manubhai Trivedi, and Thomas B Moeslund. Vision-based traffic sign detection and analysis for intelligent driver assistance systems: Perspectives and survey. *IEEE Transactions on Intelligent Transportation Systems*, 13(4), 2012. 4
- Xingang Pan, Jianping Shi, Ping Luo, Xiaogang Wang, and Xiaoou Tang. Spatial as deep: Spatial cnn for traffic scene understanding. In *AAAI*, volume 32, 2018. 4
- Vasili Ramanishka, Yi-Ting Chen, Teruhisa Misu, and Kate Saenko. Toward driving scene understanding: A dataset for learning driver behavior and causal reasoning. In *CVPR*, 2018. 5
- Amir Rasouli, Iuliia Kotseruba, and John K Tsotsos. Are they going to cross? a benchmark dataset and baseline for pedestrian crosswalk behavior. In *Int. Conf. Comput. Vis. Worksh.*, 2017. 4, 5
- Vladislav Igorevich Shakhuro and AS Konouchine. Russian traffic sign images dataset. *Computer optics*, 40(2), 2016. 4
- Johannes Stallkamp, Marc Schlipsing, Jan Salmen, and Christian Igel. Man vs. computer: Benchmarking machine learning algorithms for traffic sign recognition. *Neural networks*, 32, 2012. 1, 4
- Yafu Tian, Alexander Carballo, Ruifeng Li, and Kazuya Takeda. Road scene graph: A semantic graph-based scene representation dataset for intelligent vehicles. *arXiv preprint arXiv:2011.13588*, 2020. 5

- Radu Timofte, Karel Zimmermann, and Luc Van Gool. Multi-view traffic sign detection, recognition, and 3d localisation. *Machine vision and applications*, 25, 2014. 4
- TuSimple. <https://github.com/TuSimple/tusimple-benchmark>, 2017. 4
- Benjamin Wilson, William Qi, Tanmay Agarwal, John Lambert, Jagjeet Singh, Siddhesh Khandelwal, Bowen Pan, Ratnesh Kumar, Andrew Hartnett, Jhony Kaesemodel Pontes, et al. Argoverse 2: Next generation datasets for self-driving perception and forecasting. *arXiv preprint arXiv:2301.00493*, 2023. 6
- Tao Wu and Ananth Ranganathan. A practical system for road marking detection and recognition. In *2012 IEEE intelligent vehicles symposium*. IEEE, 2012. 4
- Hang Xu, Shaoju Wang, Xinyue Cai, Wei Zhang, Xiaodan Liang, and Zhenguo Li. Curvelane-nas: Unifying lane-sensitive architecture search and adaptive point blending. In *ECCV*. Springer, 2020. 4
- Fan Yan, Ming Nie, Xinyue Cai, Jianhua Han, Hang Xu, Zhen Yang, Chaoqiang Ye, Yanwei Fu, Michael Bi Mi, and Li Zhang. Once-3dlanes: Building monocular 3d lane detection. In *CVPR*, 2022. 1, 2
- Fisher Yu, Haofeng Chen, Xin Wang, Wenqi Xian, Yingying Chen, Fangchen Liu, Vashisht Madhavan, and Trevor Darrell. Bdd100k: A diverse driving dataset for heterogeneous multitask learning. In *CVPR*, 2020. 2, 4
- Zhe Zhu, Dun Liang, Songhai Zhang, Xiaolei Huang, Baoli Li, and Shimin Hu. Traffic-sign detection and classification in the wild. In *CVPR*, 2016. 4